This document is downloaded from DR-NTU (https://dr.ntu.edu.sg)
Nanyang Technological University, Singapore.

Highly Stable Transparent Conductive Silver Grid/PEDOT:PSS Electrodes for Integrated Bifunctional Flexible Electrochromic Supercapacitors

Cai, Guofa; Darmawan, Peter; Cui, Mengqi; Wang, Jiangxin; Chen, Jingwei; Magdassi, Shlomo; Lee, Pooi See

2015

Cai, G., Darmawan, P., Cui, M., Wang, J., Chen, J., Magdassi, S., et al. (2016). Highly Stable Transparent Conductive Silver Grid/PEDOT:PSS Electrodes for Integrated Bifunctional Flexible Electrochromic Supercapacitors. Advanced Energy Materials, 6, 1501882-.

https://hdl.handle.net/10356/80590

https://doi.org/10.1002/aenm.201501882

© 2015 WILEY-VCH Verlag GmbH & Co. KGaA, Weinheim. This is the author created version of a work that has been peer reviewed and accepted for publication by Advanced Energy Materials, WILEY-VCH Verlag GmbH & Co. KGaA, Weinheim. It incorporates referee’s comments but changes resulting from the publishing process, such as copyediting, structural formatting, may not be reflected in this document. The published version is available at: [http://dx.doi.org/10.1002/aenm.201501882].

Downloaded on 24 Aug 2022 21:10:51 SGT

Submitted to ADVANCED ENERGY MATERIALS

DOI: 10.1002/aenm.((please add manuscript number))

Highly Stable Transparent Conductive Silver Grid/PEDOT:PSS Electrodes for Integrated Bifunctional Flexible Electrochromo-Supercapacitor

*By Guofa Cai,[†] Peter Darmawan,[†] Mengqi Cui, Jiangxin Wang, Jingwei Chen, Shlomo Magdassi, and Pooi See Lee**

[*] G. F. Cai, P. Darmawan, M. Q. Cui, J. X. Wang, J. W. Chen, Prof. P. S. Lee
School of Materials Science and Engineering
50 Nanyang Avenue
Nanyang Technological University
Singapore, 639798
E-mail: pslee@ntu.edu.sg
Prof. S. Magdassi
Institute of Chemistry and the Center for Nanoscience and Nanotechnology
The Hebrew University of Jerusalem
Jerusalem, 91904, Israel
[†]These authors contributed equally to this work.

Keywords: electrochromo-supercapacitor, flexible transparent electrode, silver grid, electrochromism, energy storage

Abstract

Silver grids are attractive for replacing indium tin oxide as flexible transparent conductors. This work aims to tackle the looming concern of electrochemical stability of silver based transparent conductors. The silver grid/PEDOT:PSS hybrid film with high conductivity and excellent stability has been successfully fabricated. We demonstrate its functionality for flexible electrochromic applications by coating one layer WO_3 nanoparticles on the silver grid/PEDOT:PSS hybrid film. It presents a large optical modulation of 81.9% at 633 nm, fast switching and high coloration efficiency (124.5 cm^2 C^{-1}). More importantly, excellent electrochemical cycling stability (sustaining 79.1% of their initial transmittance modulation after 1,000 cycles) and remarkable mechanical flexibility (optical modulation decays 7.5% after compressive bending 1,200 cycles) were achieved. We present a novel smart supercapacitor which functions as a regular energy storage device and simultaneously monitors the level stored

energy by rapid and reversible color variation even at high current charge/discharge conditions. The film sustains an optical modulation of 87.7% and a specific capacitance of 67.2 % at 10 A g^{-1} compared with their initial value at the current density of 1 A g^{-1}, respectively. The high-performance silver grid/PEDOT:PSS hybrid transparent films exhibit promising features for various emerging flexible electronics and optoelectronics device.

1. Introduction

Supercapacitor offers a number of desirable properties when compared with conventional batteries, such as rapid charging/discharging rate, high power density, superior rate capability and long terms stability.[1-3] Major progress has been achieved in the theoretical and practical aspects of supercapacitors in recent years.[4-6] Meanwhile, supercapacitors with more functions and novel features have been sought to extend the application range. For example, the flexible, stretchable and wearable supercapacitors were developed to meet the requirements in the portable and wearable electronics.[7-10] Especially, it is highly attractive to integrate energy storage and electrochromism function into one device for multiple applications. Such device could be used not only for energy storage smart window which can store energy by charging the window and adjusting the light and heat of the building,[11, 12] but also for sensing variations in the level of stored energy and being able to respond to the variations in a noticeable and predictable manner.[13-16] As a key component of these smart devices, the transparent electrodes require not only high transparency but also high conductivity to simultaneously meet the needs of charging/discharging under high current density conditions and fast coloration switching speed. However, the most commonly used transparent conducting electrodes are indium tin oxide (ITO) coated glass,[11, 16] fluorine tin oxide (FTO) coated glass,[13, 15] poly (3,4-

ethylenedioxythiophene)–poly(styrene sulfonate) (PEDOT:PSS)[12] and carbon nanotubes [14]. The sheet resistance of these transparent conducting electrodes is in the range of decades to hundreds Ω/square which could hinder the device charging/discharging process and lead to the color changes lag behind the changes of the stored energy, especially under high current density. In addition, ITO and FTO as transparent electrodes are unsuitable for flexible electronics application due to their brittleness and high-cost of the preparation procedure.[17-19] Therefore, it is very important to design an electrode with a low electrical resistance and a high optical transmittance for smart energy storage device application.

A variety of flexible transparent electrodes have been investigated as an ideal low cost ITO substitute, including conducting polymers,[20] carbon nanotubes (CNTs),[21] graphene,[22] metal nanowires [23, 24] or metal grid [25-27]. Among these flexible transparent electrodes, silver grid transparent electrode is of particular interest because of its high conductivity and the high transparency realized through percolating grids. However, the silver based (e.g. nanowire, grid et al.) transparent electrodes suffer from poor cycling stability for electrochromic application due to the oxidation and corrosion of silver under positive potential in electrolyte.[28-30] So far, there are no reports on the use of metal transparent electrode for supercapacitor application. Recently, Cui's group[31] developed the silver and copper nanowires based flexible transparent electrodes by fully encapsulating large-area monolayer graphene film via roll-to-roll method. With protection of encapsulated graphene layer on silver nanowires, the cycling stability of the transparent electrode is enhanced when used for electrochromic application. However, the encapsulation process is complex and expensive. Although some work has been conducted on fabricating silver-PEDOT:PSS composite to enhance transparency, conductivity and stability in

air,[32-36] there is lack of comprehensive research on electrochemical applications, such as supercapacitor, electrochromism and electrocatalysis et al.

Herein, we introduce a simple and low cost method to enhance the electrochemical stability of silver grid/polyethylene terephthalate (PET) transparent electrode by over coating one layer of PEDOT:PSS. The silver grid/PEDOT:PSS electrode exhibits excellent performance with a low sheet resistance of 0.62 Ω/sq at over 70% transparency, excellent rate capability and high stability when it is used for electrochromic and supercapacitor electrode. We demonstrate an electrochromo-supercapacitor based on silver grid/PEDOT:PSS electrode in which the rapid and reversible color variation can response to the change on the level of stored energy even at high current charge/discharge conditions.

2. Results and Discussion

2.1 Microstructure characteristics

Figure 1a schematically illustrates the detail structure of the transparent, conductive, and flexible silver grid/PEDOT:PSS hybrid film. A representative scanning electron microscopy (SEM) image of the silver grid/PEDOT:PSS hybrid film is presented in Figure 1b. From the low magnification image, there is no obvious difference between the silver grid/PEDOT:PSS hybrid film and pristine uncoated silver grid (Figure S1 in Supporting Information). The film retains its original grid structure after coating the PEDOT:PSS. At higher magnification of the silver grid/PEDOT:PSS hybrid film, it can be seen that all silver particles are coated by the PEDOT:PSS. The voids between the silver particles in the hybrid film are bridged by the conductive PEDOT:PSS polymer which could improve the electrical conductivity. The energy dispersive X-ray spectroscopy (EDS) mapping was performed to further confirm the uniform

distribution of PEDOT:PSS by tracing the sulfur element which only belongs to the PEDOT:PSS as shown in Figure 1c. Usually, the silver grid shows slow and uneven electrochromics switching (blooming effect) due to interfacial resistance and inhomogeneity in lateral charge transport. The differences in surface resistance leading to areas in close proximity to the metal grid lines responding faster than those in the center of a grid.[27] The PEDOT:PSS coated on the silver grid not only improves the conductivity of the electrode but also reduces the blooming effect significantly. Atmospheric corrosion is an important concern for metal based transparent conducting electrodes which may hinder the practical applications. Introducing a corrosion-inhibiting coating onto the metal based transparent conducting electrodes appears to be an effective solution to resolve this issue. Figure 1d shows the changes in resistances in an uncovered silver grid film and a silver grid/PEDOT:PSS hybrid film upon exposure in air for 2 months. The ambient temperature and humidity for the test are around 25 °C and 65% RH, respectively. Although the sheet resistance of the fresh uncovered silver grid is as small as 0.69 Ω/sq, it increases rapidly with increasing exposure time in air (up to 0.90 Ω/sq after 2 months). However, after coating one layer PEDOT:PSS, the formed hybrid film become completely impervious to oxygen and moisture. The resistance of the hybrid film is 0.62 Ω/sq and it remained with minute fluctuation amplitude within 0.02 Ω/sq around 0.60 Ω/sq through a monitoring duration of two months, which is near measurement error. The excellent atmospheric corrosion resistance of the silver grid/PEDOT:PSS hybrid film can be attributed to the full coating of PEDOT:PSS passivation layer. In addition to the excellent atmospheric corrosion resistance and electrical property, the silver grid/PEDOT:PSS hybrid film exhibits satisfactory transmittance of over 73% within a broad spectrum from 400~800 nm as shown in Figure 1e. After coating PEDOT:PSS, the transmittance of the film reduce only 2%. A digital photo of the

silver grid/PEDOT:PSS hybrid film with a size about 7×7 cm^2 lighting up two LED indicators is shown in the inset of Figure 1e.

To fabricate the electrochomic electrode, WO_3 films were electrodeposited onto the pristine uncoated silver grid and silver grid/PEDOT:PSS hybrid films with applying a potential of −0.7 V (vs.Ag/AgCl) for 900 s as shown in Figure S2. Both films show similar current-time response during electrodeposition, the current density rapidly increased at initial stage and then to a constant value. However, a higher current density for deposition process on silver grid/PEDOT:PSS hybrid films is observed as compared to the pristine uncoated silver grid, attributed to the higher conducting active surfaces for electrochemical reaction. Uniform WO_3 nanoparticles were electrodeposited onto the surface of silver grid/PEDOT:PSS hybrid film as shown in **Figure 2a**. It is noticeable that the WO_3 nanoparticles only covered the surface of the silver grid for the pristine uncoated silver grid sample (Figure 2b). The size of the WO_3 nanoparticles electrodeposited on silver grid/PEDOT:PSS hybrid film is 10~40 nm, which is smaller than that of nanoparticles electrodeposited on pristine uncoated silver grid. X-ray photoelectron spectroscopy (XPS) measurements were used to analyze the oxidation state and binding energy of the WO_3 on silver grid/PEDOT:PSS hybrid film. Figure 2c shows the high resolution XPS spectrum of W4f. The spin–orbit doublets in this spectrum corresponding to $W4f_{7/2}$, $W4f_{5/2}$ and $W5p_{3/2}$ peaks which are located at 35.6 eV, 37.7 eV and 41.4 eV, respectively. It verifies that W in the films is at the highest oxidation state of W^{6+}, which is consistent with those reported in previous literatures for WO_3.[37-39]

2.2 Electrochemical and elctrochromic performance evaluations

The cyclic voltammetry (CV) measurements of WO_3 on uncovered silver grid and silver grid/PEDOT:PSS hybrid film were conducted with a three-electrode configuration as shown in

Figure 3a. A typical redox peak of WO_3 is observed in the CV curves, which can be ascribed to insertion (extraction) of H^+ into (out from) the WO_3. This insertion (extraction) process can be described as:

$$WO_3 + xH^+ + xe^- \leftrightarrow H_xWO_3 \quad (1)$$

Insertion of H^+ leads to reduction of W^{6+} ions to lower valence states. This leads to a color change of the WO_3 film and a dark blue color is observed when a negative bias potential applied on the film. When a positive bias potential is applied on the film, the reduced W-ions are oxidized back to the higher valence states which are accompanied by color loss due to the extraction of H^+ from the WO_3 film. The color of the film changes between transparent (bleached state) to dark blue (colored state) reversibly.The normalized area of the hysteresis curves and the position of anodic and cathodic peaks are closely related to the charge stored in the electrochemical processes at the surface of the electrodes. It can be seen that the cathodic and anodic peak current densities of the WO_3 on silver grid/PEDOT:PSS hybrid film are much higher than those of the WO_3 on uncovered silver grid film. This may indicate that the silver grid/PEDOT:PSS hybrid film may contain more WO_3 nanoparticles or more effective electrochemical interaction exists. The transmittance spectrum of WO_3 on uncovered silver grid film and silver grid/PEDOT:PSS hybrid film in colored and bleached states are measured under applied potential of –0.7 V and 0.1 V, respectively, as shown in Figure 3b. The WO_3 on pristine uncoated silver grid film did not show measurable contrast due to the discontinuous distribution of WO_3, specifically only on the surface of the silver particles. The silver grid/PEDOT:PSS hybrid film without deposition of WO_3 only presents a small optical modulation of 3.9% at 633 nm as shown in Figure S3 due to the electrochemical reaction of the PEDOT:PSS, that is $PEDOT^+ \cdot PSS^- + H^+ + e^- \leftrightarrow PEDOT^0 \cdot PSS^- \cdot H^+$. The WO_3 on silver grid/PEDOT:PSS hybrid film

presents a noticeable electrochromism with an optical modulation up to 81.9% at 633 nm which is highly desirable in the electrochromic devices. The optical modulation value of 81.9% is comparable to that of the single-crystalline WO_3 coated on FTO glass (85%),[39] but much higher than that of WO_3 film obtained by evaporating WO_3 powder on FTO (76.2%)[40] and electrodepositing macroporous WO_3 arrays on ITO glass (52%) [41]. In addition, only a few of research groups have reported an optical modulation of over 80% for WO_3 nanomaterial so far.[29, 39] The digital photos of WO_3 on silver grid/PEDOT:PSS hybrid film under bleached state and colored state are shown in the inset of Figure 3b. The switching time from one state to another state under alternating potentials is an important parameter for electrochromic application, which is also a direct indicator for the kinetics in electrochemical process. The switching time is defined as the time required for a system to reach 90% of the transmittance change between the steady bleached and colored states. Figure 3c and d reveal the chronoamperometry (CA) measurements and the corresponding in-situ transmittance at 633 nm, respectively. For the WO_3 on silver grid/PEDOT:PSS hybrid film, the switching time is 2.8 and 1.9 s for bleaching and coloration respectively, which is comparable to our previous work on reflective electrochromic film based on silver nanowire (4 and 1 s),[42] but much faster than that of silver grid film (120 and 6.8 s).[29] These fast switching speeds are attributed to the low sheet resistance and uniform electric field distribution in silver grid/PEDOT:PSS hybrid film electrode. Coloration efficiency (CE) is defined as the change in optical density (ΔOD) per unit charge (ΔQ) inserted into (or extracted from) the electrochromic film, that is $CE= \Delta OD/\Delta Q=\log(T_b/T_c)/\Delta Q$, where T_b and T_c denote the transmittance in bleached and colored states at a certain wavelength. Both OD and CE represent the ability of optical modulation during the insertion (extraction) of ions into (out from) electrochromic film, but CE is under the consideration of energy consumption. A high CE

indicates that the electrochromic film exhibits large optical modulation with a small charge insertion or extraction. The plot of OD as a function of inserted charge density at a wavelength of 633 nm during coloration process is shown in Figure 3e. The CE can be calculated from the slope of the curve. The WO_3 on silver grid/PEDOT:PSS hybrid film exhibits a high CE of 124.5 cm^2 C^{-1}. The CE value of 124.5 cm^2 C^{-1} is larger than that of previous reported WO_3 nanomaterials, which typically ranges from 20 to 103 cm^2 C^{-1}.[43-45] This result suggests the great improvement in charge utilization of the coated WO_3 nanoparticles on highly conductive silver grid/PEDOT:PSS hybrid film. Besides switching speed and CE, cycling stability is also one of the most important parameter to evaluate the electrochemical stability. Figure 3f shows the colored and bleached transmittance graph at 633 nm, which vary as a function of cycle number. The WO_3 on silver grid/PEDOT:PSS hybrid film sustains a transmittance modulation of about 79.1% of their initial value after subjected for 1,000 cycles, and sustains a transmittance modulation of about 67.3% of the initial state even when subjected to 2,000 cycles. The cycling stability is comparable to the PEDOT coated fully encapsulated graphene/silver nanowire substrate (80% of transmittance sustains after 1000 cycles),[31] but much better than that of the previous reported silver based substrate, [27, 29, 30, 46] which typically stabilize for several or dozens of cycles. Considering the harsh conditions such as strong oxidizing agent of H_2SO_4 and positive potential during the cycling, the silver grid/PEDOT:PSS hybrid film still retains good cycling stability, indicating that the PEDOT:PSS has successfully protected the silver grid as an effective passivation layer.

To investigate the mechanical stability, the transmittances of the WO_3 on silver grid/PEDOT:PSS hybrid film at bleached and colored state were monitored as a function of the number of bending cycles under both compressive and tensile bending tests with curvature radius

of 20 mm. It can be seen from **Figure** 4a and b that the optical modulation only decays 7.5% after compressive bending cycles of up to 1,200 times. In addition, the optical modulation with 20% degradation after tensile bending cycles of up to 800 times is shown in Figure 4c and d. These results presented here illustrate that the WO_3 on silver grid/PEDOT:PSS hybrid film possesses outstanding flexibility and mechanical durability. The high flexibility and mechanical durability of the hybrid film are essential in the emerging flexible electronics development.

The above results demonstrate that the WO_3 on silver grid/PEDOT:PSS hybrid film exhibits excellent electrochromic performance. In addition, both the electrochromic and the supercapacitive behavior of WO_3 are due to the redox reactions between W^{6+} and W^{5+} in the same electrolyte as described in reaction (1). It is very interesting to combine supercapacitive and electrochromic effects to develop an energy storage device which is capable to sense changes in the level stored energy and can monitor these changes by visual contrast even under high current charge/discharge conditions. However, the color change is required to be sufficiently rapid for observation especially at high current charge/discharge process which calls for the development of highly conductive transparent electrode as the current collector. To examine the silver grid/PEDOT:PSS hybrid film used for electrochromo-supercapacitor, the charge/discharge curves at different current density and corresponding in situ transmittance at 633 nm were tested (**Figure** 5a, b and Figure S4). The downward lines are corresponding to charging and upward ones for discharging process. The charging and discharging processes are corresponding to the insertion and extraction of H^+ into and out from the WO_3 film. Therefore, insertion of H^+ reduced W^{6+} ions to lower valence states leads to a color change of the WO_3 film and a dark blue color is observed when charge the film. During the discharging process, the reduced W-ions are oxidized back to the higher valence states which are accompanied by color

loss due to the extraction of H^+ from the WO_3 film. When WO_3 on silver grid/PEDOT:PSS hybrid film is charged to -0.7 V, reaching a fully charged state, the color of the film turns to deep blue. In reverse process, when the discharge process is completed at a potential of 0 V, the film changes to transparent. The color change is sufficiently rapid for observation even at high current density of 10 A g^{-1} (Figure 5b). The WO_3 on silver grid/PEDOT:PSS hybrid film exhibits specific capacitance of 221.1, 195.4, 168.6, 153.1 and 148.6 F g^{-1} at 1, 2, 5, 8 and 10 A g^{-1}, respectively, which are higher than the values of previously reported WO_3 pseudocapacitive nanomaterials.[47-49] Figure 5c shows the dependence of optical modulation and specific capacitance on current density for the WO_3 on silver grid/PEDOT:PSS hybrid film. It is observed that the optical modulation and specific capacitance decrease gradually with increasing current density, which could result from that some active surface areas of the active materials which become inaccessible for charge storage due to the diffusion effect, limiting the migration of the electroactive ions at high current density. The film sustains an optical modulation and a specific capacitance of 87.7% and 67.2 % at 10 A g^{-1}, compared with their initial values at the current density of 1 A g^{-1}, respectively, indicative of excellent rate capability under high current charge/discharge conditions. In addition, the capacitance retains 54.6% even at a high current density of 5 A g^{-1} after subjected to 2000 cycles as shown in Figure S5. The WO_3 on silver grid/PEDOT:PSS hybrid film presents an effective color change during fast charge and discharge process. Therefore, we demonstrate that the states of energy storage can be visually monitored by the color change at different current density. To the best of our knowledge, this work is the first demonstration on the realization of electrochromo-supercapacitor using metal based transparent electrode.

3. Conclusions

In summary, silver grid/PEDOT:PSS hybrid film is successfully fabricated by a simple and low cost method, the hybrid film shows high conductivity with satisfactory transparency, high stability against oxidation and remarkable flexibility. Large optical modulation, fast switching, high CE and excellent cycling stability were achieved on flexible substrates when WO_3 was coated on its surface for electrochromic applications. Moreover, we have demonstrated for the first time, a novel smart supercapacitor using metal based transparent electrode in which the rapid and reversible color variation can response to the change on the level of stored energy even at high current charge/discharge conditions. With the tremendous improvements of comprehensive performance, especially the chemical stability, conductivity, mechanical flexibility and low cost, the silver grid/PEDOT:PSS hybrid film is a promising candidate for transparent conducting electrode.

Experimental Section

Preparation of hybrid silver grid/PEDOT electrode

All reagents used were analytical grade and used without additional purification. The Ag-grid used in this study is prepared by silver nanoparticles self-assembled and sintered into periodic uniform squares on a PET substrate according to our previous work.[30] The hybrid silver grid/PEDOT:PSS electrode was then obtained by spin-coating PEDOT:PSS (1.3 wt% dispersion in H_2O, purchased from Sigma-Aldrich) on to the silver grid/PET film. The spin coating processes were performed firstly at 800 rpm for 8 s and then at 2000 rpm for 30 s. The film was then heated at 135 °C for 30 min for the PEDOT:PSS curing. The WO_3 film was coated

on the surface of silver grid/PEDOT:PSS electrode by cathodic electrodeposition according to the literature.[50] The loading mass was 0.34 mg cm^{-2} when the electrodeposition process was conducted at a potential of −0.7 V (vs.Ag/AgCl) for 900 s. For comparison, the WO_3 film on a silver grid/PET substrate was also prepared with the same parameters.

Sample characteristics

The SEM (JEOL 7600F) and EDS mapping were used to characterize the morphology, structure and composition of the film. XPS analysis of the WO_3 film was performed using the VG ESCALab 220i-XL Imaging XPS. The maximum analysis depth lay in the range of 4 – 8 nm. The error of binding energy is estimated to be within ± 0.2 eV. The transmittance and sheet resistance of films were measured by a SHIMADZU UV-3600 spectrophotometer and a four-point probe (JANDEL RM3000), respectively. Each reported value of the sheet resistance is the average of 5 measurement points. The electrochromic and electrochemical measurements were conducted in a three–electrode electrochemical cell containing 0.5 M H_2SO_4 aqueous solution as the electrolyte. CV measurements were performed on a Solartron 1470E at 20 mV s^{-1} between -0.7 V and 0.1 V with the Ag/AgCl as the reference electrode and Pt foil as counter-electrode at 25 °C. Electrochromic and galvanostatic charging and discharging measurements were carried out in a three-electrode electrochemical cell, the WO_3 coated silver grid/PEDOT:PSS electrode was used as working electrode, an Ag wire was used as the reference electrode and a Pt wire was used as the counter electrode. The transmittance of the silver grid/PET substrate in the electrolyte was considered to be 100 % and was used as the baseline. The mechanical bending tests in both bending and compression (with radius of curvature 20 mm) were carried out on the WO_3 on

silver grid/PEDOT:PSS electrode. Optical modulation was measured at the bleached and colored state. The specific capacitance was calculated according to the equation (2):

$$C = \frac{I\Delta t}{M\Delta V} \quad (2)$$

Where C (F g^{-1}) is the specific capacitance, I (mA) denotes the discharge current, and Δt (sec), M (mg) and ΔV (V) represent the total discharge time, mass of active materials and potential drop during discharge, respectively.

Supporting Information
Supporting Information is available online from the Wiley Online Library or from the author.

Acknowledgements
This research is supported by NRF Competitive Research Programme NRF-CRP13-2014-02. Part of the work is also supported by A*Star-MND Green Building Joint Grant 1321760013, and NTU-HUJ-BGU Nanomaterials for Energy and Water Management Programme under the Campus for Research Excellence and Technological Enterprise (CREATE) that is supported by the National Research Foundation, Prime Minister's Office, Singapore. We acknowledge M. Layani for providing the metal particles.

Received: ((will be filled in by the editorial staff))
Revised: ((will be filled in by the editorial staff))
Published online: ((will be filled in by the editorial staff))

[1] P. Simon, Y. Gogotsi, *Nat. Mater.* **2008**, *7*, 845.

[2] A. Sumboja, C. Y. Foo, X. Wang, P. S. Lee, *Adv. Mater.* **2013**, *25*, 2809.

[3] D. S. Yu, K. Goh, H. Wang, L. Wei, W. C. Jiang, Q. Zhang, L. M. Dai, Y. Chen, *Nat. Nano.* **2014**, *9*, 555.

[4] X. Wang, C. Y.Yan, A. Sumboja, J. Yan, P. S. Lee, *Adv.Energy Mater.* **2014**, *4*, 1301240.

[5] H. Jiang, J. Ma, C. Z. Li, *Adv. Mater.* **2012**, *24*, 4197.

[6] X. H. Lu, M. H. Yu, G. M. Wang, T. Zhai, S. L. Xie, Y. C. Ling, Y. X. Tong, Y. Li, *Adv. Mater.* **2013,** *25*, 267‑272.

[7] S. Y. Hong, J. Yoon, S. W. Jin, Y. Lim, S.-J. Lee, G. Zi, J. S. Ha, *ACS Nano* **2014**, *8*, 8844.

[8] T. Chen, R. Hao, H. S. Peng, L. M. Dai, *Angew. Chem. Int. Ed.* **2015**, *54*, 618.

[9] C. Choi, S. H. Kim, H. J. Sim, J. A. Lee, A. Y. Choi, Y. T. Kim, X. Lepro, G. M. Spinks, R. H. Baughman, S. J. Kim, *Sci. Rep.* **2015**, *5,* 9387.

[10] L. B. Liu, Y. Yu, C. Yan, K. Li, Z. J. Zheng, *Nat. Commun.* **2015**, *6,7260*.

[11] Z. Xie, X. J. Jin, G. Chen, J. Xu, D. Chen, G. Z. Shen, *Chem. Commun.* **2014**, *50*, 608.

[12] K. Wang, H. P. Wu, Y. N. Meng, Y. J. Zhang, Z. X. Wei, *Energy Environ. Sci.* **2012**, *5*, 8384.

[13] D. Wei, M. R. J. Scherer, C. Bower, P. Andrew, T. Ryhänen, U. Steiner, *Nano Lett.* **2012**, *12*, 1857.

[14] X. L. Chen, H. J. Lin, P. N. Chen, G. Z.Guan, J. Deng, H. S. Peng, *Adv. Mater.* **2014**, *26*, 4444.

[15] Y. Y. Tian, S. Cong, W. M. Su, H. Y. Chen, Q. W. Li, F. X. Geng, Z. G. Zhao, *Nano Lett.* **2014**, *14*, 2150.

[16] G. F. Cai, X. Wang, M. Q. Cui, P. Darmawan, J. X. Wang, A. L.-S. Eh, P. S. Lee, *Nano Energy* **2015**, *12*, 258.

[17] K. Ellmer, *Nat. Photon.* **2012**, *6*, 809.

[18] Y. H. Kim, L. Müller-Meskamp, K. Leo, *Adv. Energy Mater.* **2015**, *5*, 1401822.

[19] A. Kumar, C. Zhou, *ACS Nano* **2010**, *4*, 11.

[20] S. Shin, M. Y. Yang, L. J. Guo, H. Youn, *Small* **2013**, *9*, 4036.

[21] H. S. Peng, *J. Am. Chem. Soc.* **2008**, *130*, 42.

[22] K. S. Kim, Y. Zhao, H. Jang, S. Y. Lee, J. M. Kim, K. S. Kim, J.-H. Ahn, P. Kim, J.-Y. Choi, B. H. Hong, *Nature* **2009**, *457*, 706.

[23] J. Z.Song, J. H. Li, J. Y. Xu, H. B. Zeng, *Nano Lett.* **2014,** *14*, 6298.

[24] Y. X. Jin, L. Li, Y. R. Cheng, L. Q. Kong, Q. B. Pei, F. Xiao, *Adv. Funct. Mater.* **2015**, *25*, 1581.

[25] J. H. Park, D. Y. Lee, W. Seung, Q. Sun, S.-W. Kim, J. H. Cho, *J. Phys. Chem. C* **2015**, *119*, 7802.

[26] L. Mao, Q. Chen, Y. W. Li, Y. Li, J. H. Cai, W. M. Su, S. Bai, Y. Z. Jin, C.-Q. Ma, Z. Cui, L. W. Chen, *Nano Energy* **2014**, *10*, 259.

[27] J. Jensen, M. Hösel, I. Kim, J.-S. Yu, J. Jo, F. C. Krebs, *Adv. Funct. Mater.* **2014**, *24*, 1228.

[28] J. Jensen, F. C. Krebs, *Adv. Mater.* **2014**, *26*, 7231.

[29] L. Liu, M. Layani, S. Yellinek, A. Kamyshny, H. Ling, P. S. Lee, S. Magdassi, D. Mandler, *J. Mater. Chem. A* **2014**, *2*, 16224.

[30] M. Layani, P. Darmawan, W. L. Foo, L. Liu, A. Kamyshny, D. Mandler, S. Magdassi, P. S. Lee, *Nanoscale* **2014**, *6*, 4572.

[31] B. Deng, P.-C. Hsu, G. C. Chen, B. N. Chandrashekar, L. Liao, Z. Ayitimuda, J. X. Wu, Y. Guo, L. Lin, Y. Zhou, M. Aisijiang, Q. Xie, Y. Cui, Z. F. Liu, H. L. Peng, *Nano Lett.* **2015**, *15*, 4206.

[32] S. Kim, S. Y. Kim, J. Kim, J. H. Kim, *J. Mater. Chem. C* **2014**, *2*, 5636.

[33] S. Chen, L. Song, Z. Tao, X. Shao, Y. Huang, Q. Cui, X. Guo, *Org. Electron.* **2014**, *15*, 3654.

[34] Q. J. Xu, T. Song, W. Cui, Y. Q. Liu, W. D. Xu, S.-T. Lee, B. Q. Sun, *ACS Appl. Mater. Interfaces* **2015**, *7*, 3272.

[35] Y.-S. Kim, M.-H. Chang, E.-J. Lee, D.-W. Ihm, J.-Y. Kim, *Synth. Met.* **2014**, *195*, 69.

[36] Y.-J. Noh, S.-S. Kim, T.-W. Kim, S.-I. Na, *Sol. Energy Mater. Sol. Cells* **2014**, *120, Part A*, 226.

[37] G. F. Cai, X. L. Wang, D. Zhou, J. H. Zhang, Q. Q. Xiong, C. D. Gu, J. P. Tu, *Rsc Adv.* **2013**, *3*, 6896.

[38] A. Benoit, I. Paramasivam, Y. C. Nah, P. Roy, P. Schmuki, *Electrochem. Commun.* **2009**, *11*, 728.

[39] S. Cong, Y. Y. Tian, Q. W. Li, Z. G. Zhao, F. X. Geng, *Adv. Mater.* **2014**, *26*, 4260.

[40] P. H. Yang, P. Sun, Z. S. Chai, L. H. Huang, X. Cai, S. Z. Tan, J. H. Song, W. J. Mai, *Angew. Chem. Int. Ed.* **2014**, *53*, 11935.

[41] J. Zhang, J. P. Tu, G. F. Cai, G. H. Du, X. L. Wang, P. C. Liu, *Electrochim. Acta* **2013**, *99*, 1.

[42] C. Y. Yan, W. B. Kang, J. X. Wang, M. Q. Cui, X. Wang, C. Y. Foo, K. J. Chee, P. S. Lee, *ACS Nano* **2013**, *8*, 316.

[43] J. Zhang, J. P. Tu, X. H. Xia, X. L. Wang, C. D. Gu, *J. Mater. Chem.* **2011**, *21*, 5492.

[44] S. H. Lee, R. Deshpande, P. A. Parilla, K. M. Jones, B. To, A. H. Mahan, A. C. Dillon, *Adv. Mater.* **2006**, *18*, 763.

[45] G. F. Cai, J.P. Tu, D. Zhou, L. Li, J. H. Zhang, X. L. Wang, C. D. Gu, *CrystEngComm* **2014**, *16*, 6866.

[46] H.-Y. Lu, C.-Y. Chou, J.-H. Wu, J.-J. Lin, G.-S. Liou, *J. Mater. Chem. C* **2015**, *3*, 3629.

[47] B. N. Reddy, P. N. Kumar, M. Deepa, *ChemPhysChem* **2015**, *16*, 377.

[48] Y. Cai, Y. Wang, S. J. Deng, G. Chen, Q. Li, B. Q. Han, R. Han, Y. D. Wang, *Ceram. Int.* **2014**, *40*, 4109.

[49] S. Yoon, E. Kang, J. K. Kim, C. W. Lee, J. Lee, *Chem. Commun.* **2011**, *47*, 1021.

[50] G. F. Cai, D. Zhou, Q. Q. Xiong, J. H. Zhang, X. L. Wang, C. D. Gu, J. P. Tu, Sol. Energy Mater. Sol. Cells **2013**, 117, 231.

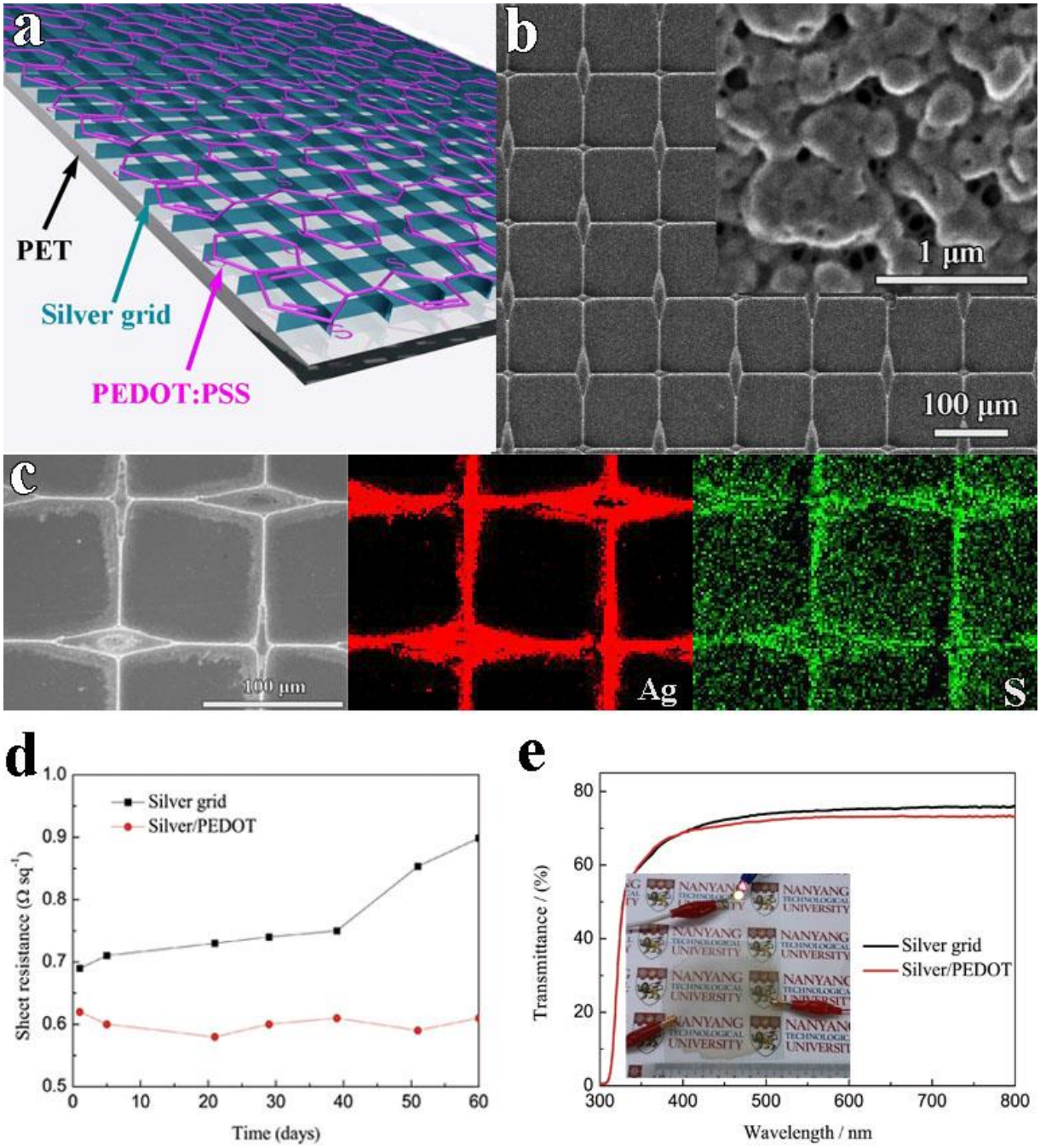

Figure 1. (a) schematic illustration of the structure of the silver grid/PEDOT:PSS hybrid film. (b) Low and high magnification SEM image of the hybrid film. (c) EDS mapping of the hybrid film, demonstrating the uniform distribution of PEDOT:PSS across the whole film. (d) Changes in sheet resistance of the uncoated silver grid and the silver grid/PEDOT:PSS hybrid films exposed in air at ambient temperature for two months. (e) Transmittance of uncoated silver grid and the silver grid/PEDOT:PSS hybrid films between 300~800 nm, inset shows that the hybrid film with size about 7×7 cm^2 can light up two LED indicators.

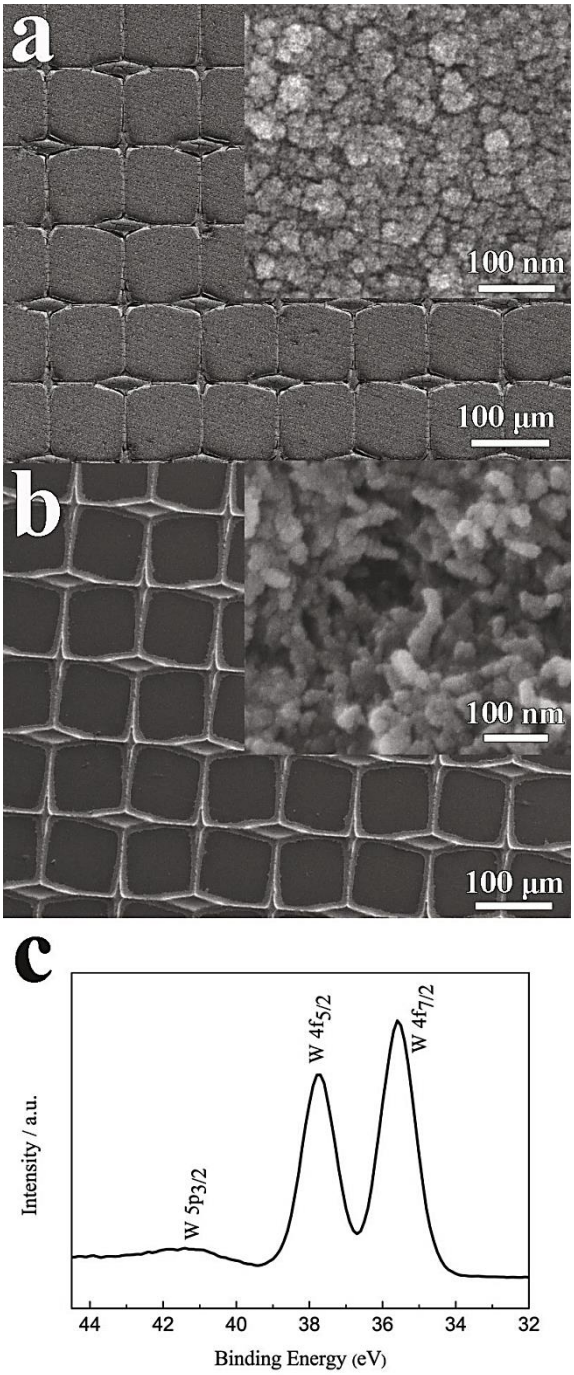

Figure 2. Low and high magnification SEM image of (a) the silver grid/PEDOT:PSS hybrid film and (b) the pristine bare silver grid after electrochemical depositing WO_3 at an applied potential of −0.7 V (vs.Ag/AgCl) for 900 s. (c) W 4f XPS spectrum of the silver grid/PEDOT:PSS hybrid film after coating WO_3 layer.

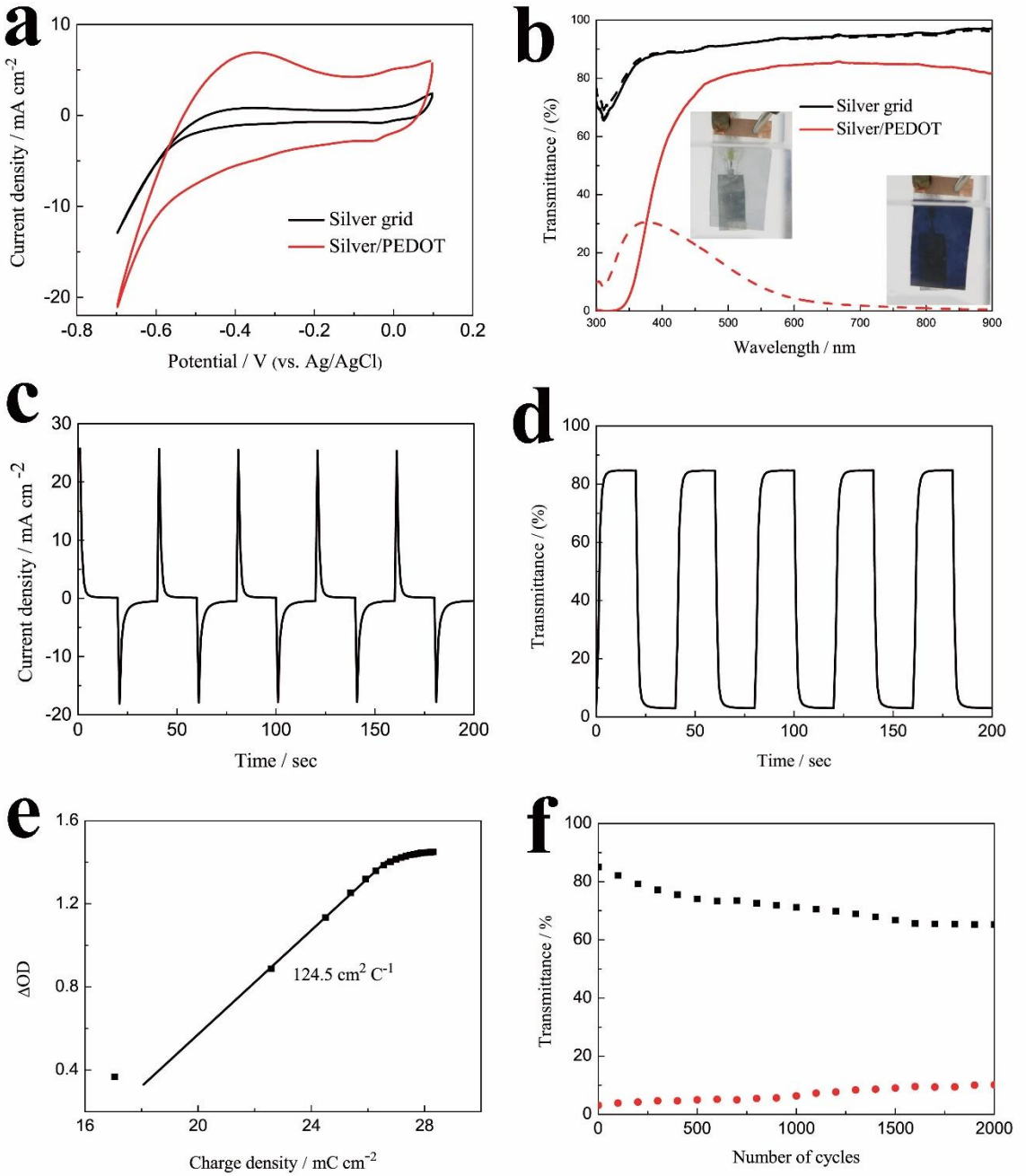

Figure 3. (a) Cyclic voltammograms of WO_3 on the pristine silver grid and the silver grid/PEDOT:PSS hybrid films in 0.5 M H_2SO_4 at a scan rates of 20 mV s^{-1} in the potential range of–0.7 to 0.1V vs. Ag/AgCl. (b) Transmittance spectra of WO_3 deposited on the pristine silver grid and the silver grid/PEDOT:PSS hybrid films in the colored (–0.7 V) and bleached (0.1 V) states between wavelength range of 300 to 900 nm. (c) Current response for the WO_3 on the silver grid/PEDOT:PSS hybrid film at 0.1 V and −0.7 V applications for 20 s per step. (d) In situ optical responses of WO_3 on the silver

grid/PEDOT:PSS hybrid film for 20 s per step measured at 633 nm. (e) Optical density variation with respect to the charge density at 633 nm. (f) Cycle performance of WO_3 on the silver grid/PEDOT:PSS hybrid film measured in 0.5 M H_2SO_4 for 2,000 cycles.

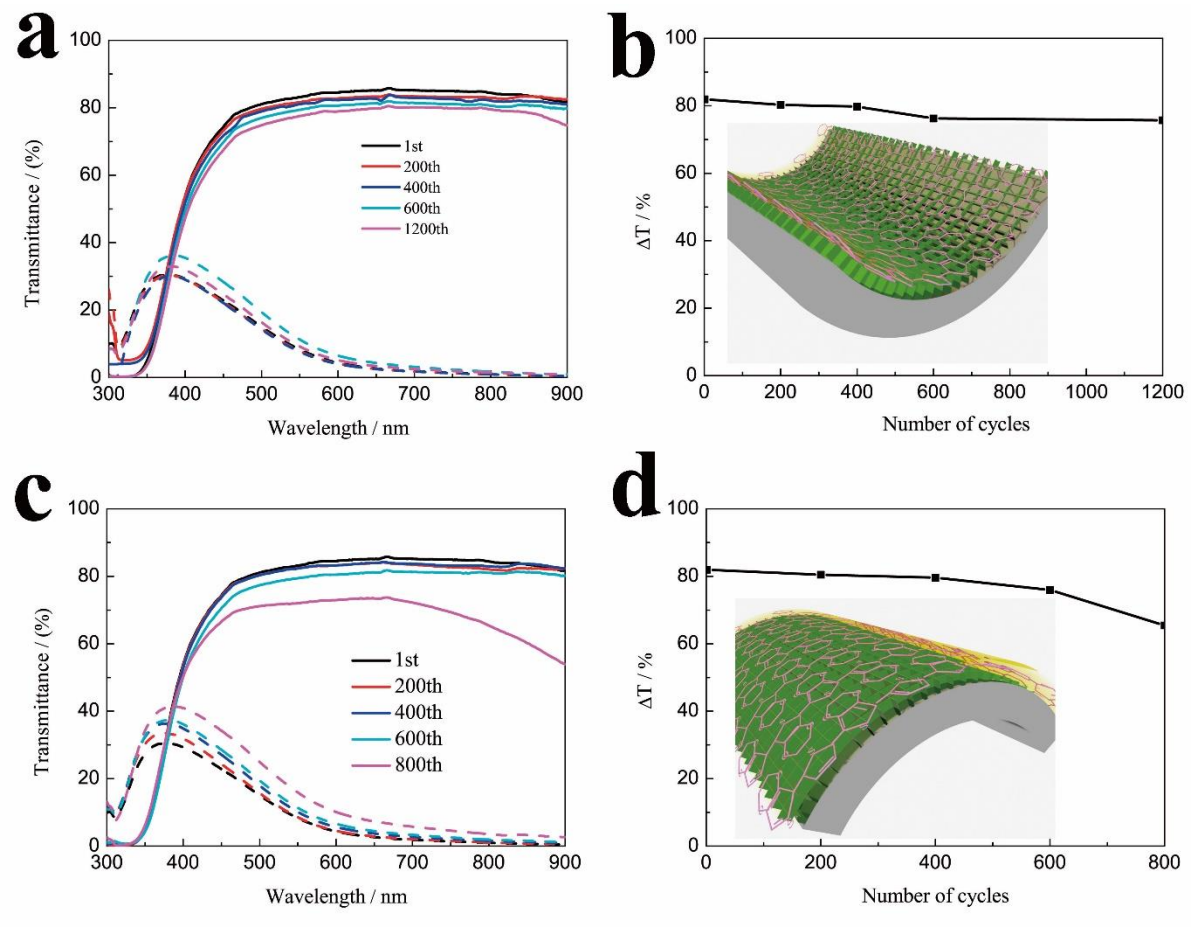

Figure 4. Transmittance and optical modulation changes of the WO_3 on silver grid/PEDOT:PSS hybrid film at bleached and colored state when suffering from repeated (a,b) compressive bending, (c,d) tensile bending with curvature radius of 20 mm.

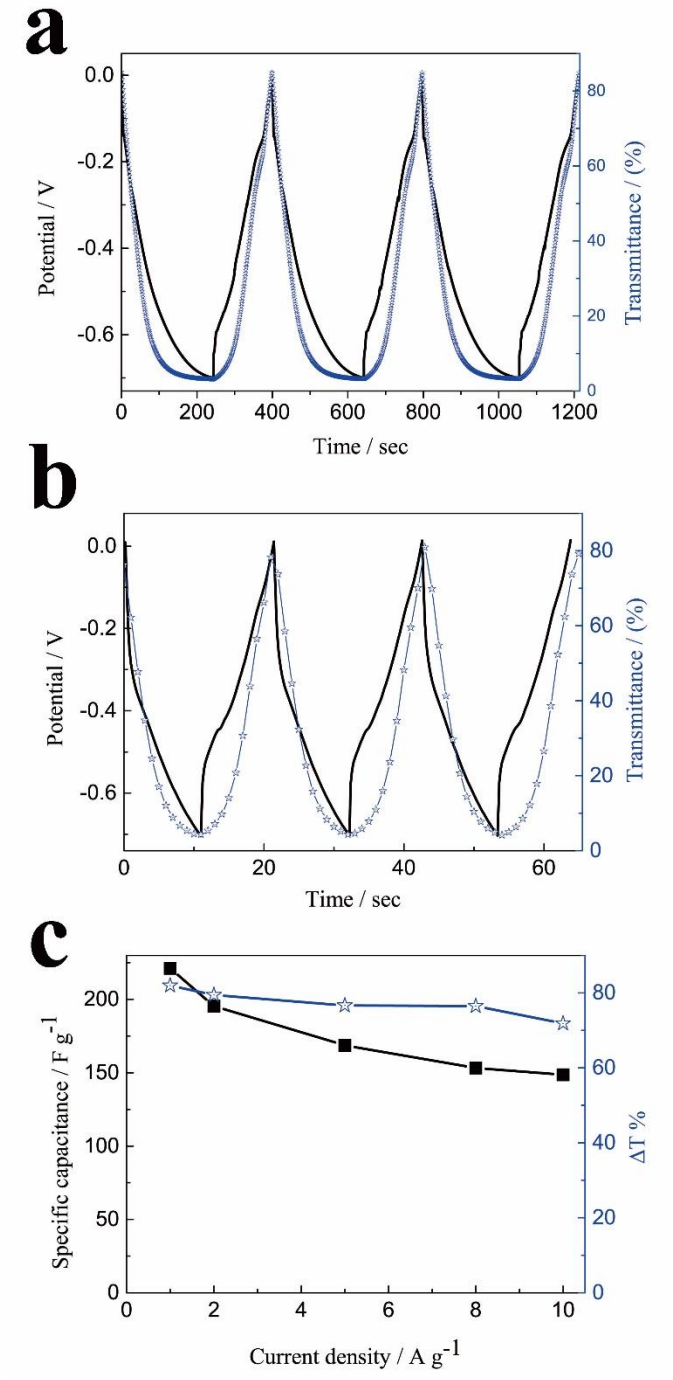

Figure 5. Galvanostatic charge/discharge profiles at (a) 1 A g^{-1} and (b) 10 A g^{-1} in the potential range of 0 to -0.7 V and corresponding in situ optical responses measured at 633 nm for the WO_3 on silver grid/PEDOT:PSS hybrid film. (c) Specific capacitance and optical modulation of the WO_3 on silver grid/PEDOT:PSS hybrid film as a function of the current density.

Table of Contents Entry

Highly stable transparent conductive silver grid/PEDOT:PSS hybrid film has been successfully fabricated by a facile and low cost method. It presents excellent electrochemical cycling stability, remarkable mechanical flexibility, outstanding electrochromic and energy storage performance when used as flexible electrochromo-supercapacitor electrodes.

Keywords

electrochromo-supercapacitor, flexible transparent electrode, silver grid, electrochromism, energy storage

Authors

*Guofa Cai,[†] Peter Darmawan,[†] Mengqi Cui, Jiangxin Wang, Jingwei Chen, Shlomo Magdassi, and Pooi See Lee **

Title

Highly Stable Transparent Conductive Silver Grid/PEDOT:PSS Electrodes for Integrated Bifunctional Flexible Electrochromo-Supercapacitor

ToC Figure (55 mm broad × 50 mm high)